

Federated Self-Supervised Contrastive Learning via Ensemble Similarity Distillation

Haizhou Shi², Youcai Zhang¹, Zijin Shen², Siliang Tang², Yaqian Li¹, Yandong Guo¹, Yueting Zhuang²

¹ OPPO Research Institute, ² Zhejiang University

{zhangyoucai, liyaqian, guoyandong}@oppo.com, {shihaizhou, zijinshen, siliang, yzhuang}@zju.edu.cn

Abstract

This paper investigates the feasibility of learning good representation space with unlabeled client data in the federated scenario. Existing works trivially inherit the supervised federated learning methods, which does not apply to the model heterogeneity and has potential risk of privacy exposure. To tackle the problems above, we first identify that self-supervised contrastive local training is more robust against the non-i.i.d.-ness than the traditional supervised learning paradigm. Then we propose a novel federated self-supervised contrastive learning framework FLESD that supports architecture-agnostic local training and communication-efficient global aggregation. At each round of communication, the server first gathers a fraction of the clients' inferred similarity matrices on a public dataset. Then FLESD ensembles the similarity matrices and train the global model via similarity distillation. We verify the effectiveness of our proposed framework by a series of empirical experiments and show that FLESD has three main advantages over the existing methods: it handles the model heterogeneity, is less prone to privacy leak, and is more communication-efficient. We will release the code of this paper in the future.

1 Introduction

Federated Learning (FL) seeks to collaboratively train the model distributed across a large network while keeping the clients' private data protected (Konecny et al. 2016; Zhao et al. 2018; Li and Wang 2019; Li et al. 2020; Lin et al. 2020; Wang et al. 2020). However, in practice, different clients may have various downstream tasks to perform. Therefore to include them in a single task-oriented supervised federated learning framework is infeasible. To fully utilize all the clients' data in a downstream-task-agnostic way, the branch of Federated Unsupervised Representation Learning (FURL) emerges, as shown in Figure 1. It aims at training a global encoder framework without annotation or violation of data-privacy (Jin et al. 2020; van Berlo, Saeed, and Ozcelebi 2020; Zhang et al. 2020).

There are three main disadvantages of current works in FURL. Firstly, they trivially inherit the current supervised federated learning frameworks such as FedAvg (McMahan et al. 2017) and fail to notice distinct properties of federated self-supervised learning (discussed in Section 2). Secondly,

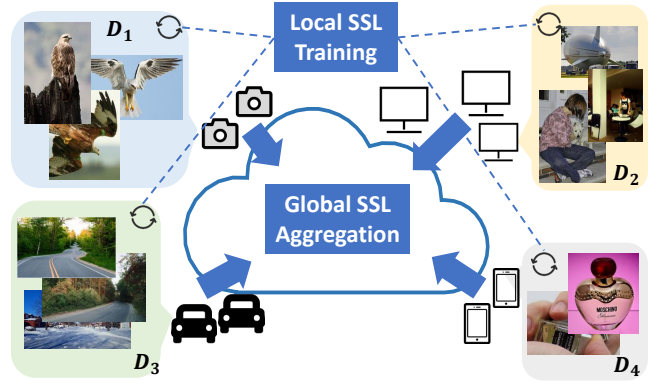


Figure 1: Federated Self-Supervised Learning on non-identically distributed (non-i.i.d.) data with model heterogeneity. In general, every round of communication consists of local training phase and global aggregation phase.

their designs are based on the weight-averaging scheme and therefore cannot scale to the model-heterogeneous federated learning systems, i.e., the model architecture varies across different clients. Thirdly, as a side-effect brought by weight averaging, they require a trustworthy third-party institution to aggregate the local model weights or otherwise has a potential hazard of privacy leaks since the local model itself carries private information.

This paper proposes to address the aforementioned three problems altogether. First, we identify an essential feature of self-supervised contrastive learning: it's more robust against the non-identically distributed (non-i.i.d., referred to as statistical heterogeneity) data across the clients, compared to supervised learning. Therefore longer epochs of local training and fewer communication rounds become viable. Next, to enable model-agnostic federated training and provide strict constraints on privacy preservation, we propose a new framework, Federated self-supervised Learning via Ensemble Similarity Distillation (FLESD). After certain epochs of local training, the clients infer the similarity matrix on a public dataset free of privacy concerns and return it to the server at each communication round. Then FLESD distills the knowledge from the ensembled similarity matrix and distributes the distilled model back to the clients.

This work was done during Haizhou's internship at OPPO.

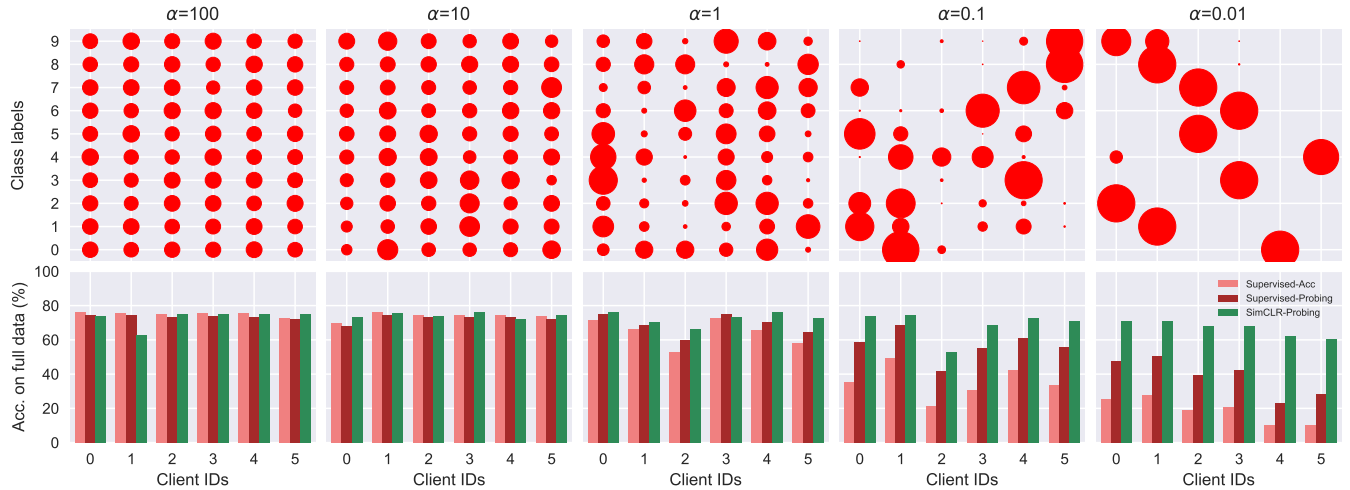


Figure 2: Local training of supervised and self-supervised learning on CIFAR10. The top row visualizes the non-i.i.d.-ness of the data distribution; the radius of each circle represents the size of the local dataset. The bottom row compares the behavior of supervised and self-supervised local training. The self-supervised framework SimCLR is more robust against non-i.i.d.-ness of the client data distribution than the supervised method. For complete demonstration on CIFAR10/CIFAR100, please refer to Figure 7. For specific statistics, please refer to Table 3.

We demonstrate with thorough empirical experiments that our method can yield good-quality representation space in a communication-efficient manner. Besides, it has the edge of aggregating knowledge from heterogeneous clients, and is less prone to privacy exposure. Our main contributions are:

- We point out that the self-supervised contrastive learning framework is robust to local training on non-i.i.d. data.
- We design a new federated self-supervised learning algorithm FLESD that possesses the edge of significantly fewer communications rounds during training, besides its strict privacy protection and feasibility in model-heterogeneous systems.
- We conduct extensive case studies on the proposed method FLESD, providing insights into its behavior.

2 Self-Supervised Contrastive Learning is Robust against Non-i.i.d. Client Data

Although self-supervised learning has proven its effectiveness when trained with a large model on the data center (Chen et al. 2020a; He et al. 2020; Grill et al. 2020; Chen and He 2020; Zbontar et al. 2021; Chen et al. 2020b; Chen, Xie, and He 2021; Chen et al. 2020c), its performance and the related properties are seldom studied in the field of federated learning. Here we answer the question of how self-supervised **local training** performs on the non-identically distributed client data (also known as non-i.i.d.-ness): what differs it from the traditional supervised learning? How can we utilize its distinct property if there is any?

Setup. As a classic self-supervised learning paradigm, we explore the behavior of SimCLR in the federated local training scenario and compare its differences between the traditional supervised learning (Chen et al. 2020a). Following Lin et al. (2020), we synthesize varying degrees of non-i.i.d.-ness by controlling the α values of the Dirichlet distribution.

The smaller α is, the less similar are the clients' local data distributions. The client number is set to $K = 6$ as it assures that some of the clients will hold only one data category when the non-i.i.d.-ness is extreme (Figure 2, $\alpha = 0.01$, client No.4, 5). The top row of Figure 2 showcases the non-i.i.d. distribution of the CIFAR10 dataset (Krizhevsky, Hinton et al. 2009) over 6 clients. The setting of SimCLR remains the same in all the experiments, i.e., backbone network set as ResNet18 (He et al. 2016), temperature $\tau = 0.4$, batch size $B = 1024$, learning rate $\eta = 1e - 3$ and is optimized for 200 epochs using Adam (Kingma and Ba 2014). The supervised method is locally trained for 100 epochs with the learning rate $\eta = 1e - 3$ and batch size $B = 128$, optimized by the Adam optimizer. To achieve a fair comparison, we evaluate the linear probing accuracy (Zhang, Isola, and Efros 2016) for both SimCLR and supervised method, i.e., we fix the backbone network and retrain a linear classifier on top of it. The accuracies of each client are reported in Figure 2.

Analysis. As the non-i.i.d.-ness increases from $\alpha = 100$ to $\alpha = 0.01$, the average accuracy of the supervised method decreases from 73.0% to 18.5% (-54.5%). The linear probing accuracy also drops drastically: from 73.5% to 38.6% (-34.9%). However, the linear probing accuracy of SimCLR remains with a subtle performance drop: from 72.8% to 66.7% (-6.1%). Even when the client holds only one single data category, which causes the supervised model to fail, SimCLR's performance maintains at an acceptable level (60.4% & 62.4% for client No.4 & No.5, respectively). This phenomenon indicates that self-supervised contrastive learning is more robust to the non-i.i.d.-ness of the client data.

We conjecture the main cause of the observed robustness is that the contrastive learning paradigm learns the invariance created by the random data augmentations, which is not severely influenced by lacking certain categories of

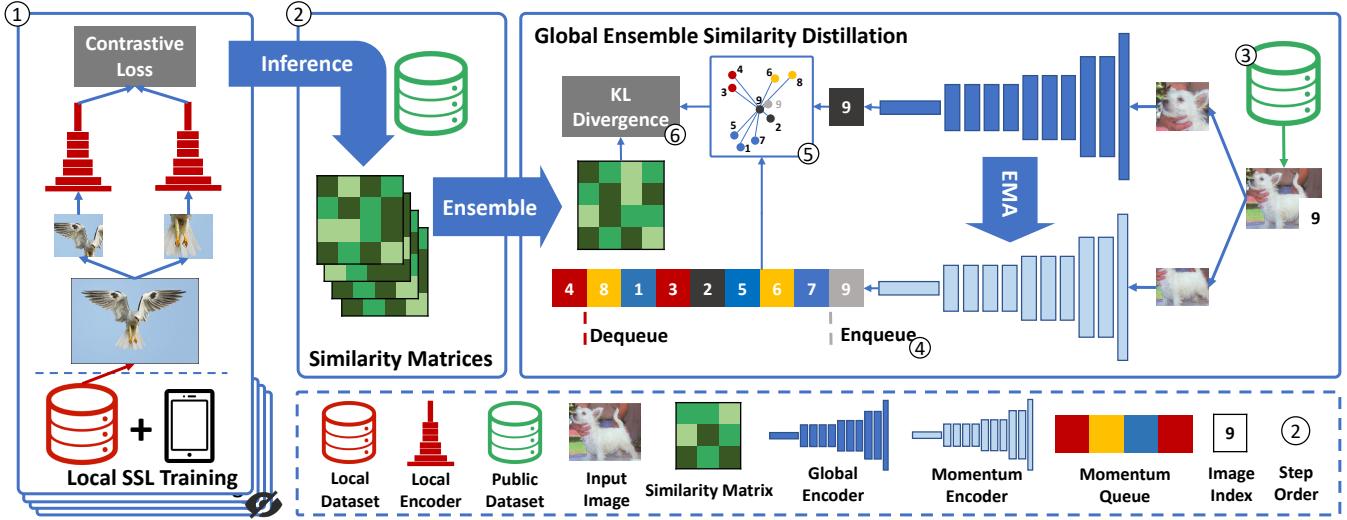


Figure 3: Federated self-supervised Learning via Ensemble Similarity Distillation (FLESD). There are three main steps during single communication round: (i) local SSL training, (ii) similarity matrix ensemble, and (iii) global ensemble similarity distillation. The specific steps are broken down and annotated in the figure: ①-local self-supervised contrastive learning; ②-similarity matrix inference and ensemble on the public dataset; ③-global aggregation on the public dataset; ④-momentum queue update; ⑤-similarity distribution calculation; ⑥-KL divergence loss calculation and model update.

data. Why and under what conditions self-supervised learning methods such as SimCLR are more robust to the non-i.i.d. data distribution is an intriguing question of its own but is beyond the scope of this paper. Nevertheless, such robustness is exploitable in federated learning since now we can aggregate the local models with an even lower frequency than federated supervised learning: the supervised counterpart often has a comparatively high communication frequency to prevent meaningless local training (Konecnuy et al. 2016; Li et al. 2020; Lin et al. 2020).

3 Methodology: FLESD

3.1 Preliminary: Federated Learning

Federated learning (FL) studies how to learn from the data examples distributed across different clients in an extensive network, with all the clients’ data privacy protected. Specifically, we seek to minimize the objective:

$$\min_w L(w) = \sum_{k=1}^K p_k L_k(w) = \mathbb{E}_k [L_k(w)], \quad (1)$$

where K is the number of the clients, $p_k \geq 0$ representing the importance of the k -th client, and $\sum_k p_k = 1$. Due to the intrinsic system and statistical heterogeneity of the varying clients, each client might have different data distribution \mathcal{D}_k and training objective l_k :

$$L_k(w) \triangleq \mathbb{E}_{x \sim \mathcal{D}_k} [l_k(x; w)]. \quad (2)$$

Unlike traditional distributed training that synchronizes the model at each local update, federated learning is often faced with the problem of network thrashing and the varying speed of local training (Konecnuy et al. 2016; Zhao et al. 2018; Li et al. 2020; Lin et al. 2020). It thus cannot be optimized in a communication-frequent manner. A commonly

adopted measure is to train each client on the local data for certain epochs and then communicate their results for model aggregation. For simplicity, this paper mainly focuses on training the local model over a unified self-supervised contrastive objective. However, our proposed method is not limited to such scenario and is applicable when varying local objectives are adopted.

3.2 Local Self-Supervised Training

Many federated systems are composed of clients that cannot provide annotations on the local data in the real world. This section describes the existing self-supervised contrastive learning that is adopted as the local training objective for the rest of the paper. Contrastive learning is motivated by the “multi-view hypothesis”, that the different views of the same data example are likely to represent a close or even the same semantics. Following Oord, Li, and Vinyals (2018), the objective l_{cl} trains the model to discern one data point’s augmented view (positive) from the rest of the data (negative):

$$l_{\text{cl}}(f) \triangleq -\mathbb{E} \left[\log \frac{e^{f(x)^\top f(x^+)/\tau}}{e^{f(x)^\top f(x^+)/\tau} + \sum_{m=1}^{M_{\text{neg}}} e^{f(x)^\top f(x_m^-)/\tau}} \right], \quad (3)$$

where f is the encoder network; x^+ is the positive view created by a series of data augmentations; x^- is the negative examples independently sampled from the data distribution, and M_{neg} represents the negative sample size. Typically, in the framework of SimCLR, the negative samples are collected from the other samples within the same batch $M_{\text{neg}} = B - 1$. As mentioned above, this training objective is applied across all the local devices, i.e., $l_k = l_{\text{cl}}, \forall k \in \{1, \dots, K\}$.

In some cases where the non-i.i.d.-ness is extreme, the local client contains only one category of the data, and the neg-

ative samples all become falsely negative. Although it leads to a certain extent of the performance decrease (as verified in Section 2), the contrastive learning objective remains to be conceptually working: it aims to discern subtle differences among the instances regardless of their semantic labels.

3.3 Global Ensemble Similarity Distillation (ESD)

Similarity matrix ensemble. To enable federated training with the model heterogeneity and pose strict constraints on the clients’ data privacy, we assume there is a publicly accessible dataset D_{pub} for the global model aggregation. Specifically, the local knowledge of the clients is extracted through the inferred similarity matrices on the public dataset.

Suppose the public dataset $|D_{\text{pub}}| = N$ has N examples. The k -th client’s representation matrix R_k is defined as $R_k \triangleq f_k(D_{\text{pub}}) \in \mathbb{R}^{d_k \times N}$, where f_k is the encoder network; the representation yielded by f_k is of d_k dimension and is automatically normalized to unit-length. The similarity matrix M_k of k -th client is computed as:

$$M_k = R_k^\top R_k, \quad (4)$$

where $M_{k,ij} = M_{k,ji} = \langle R_{k,:i}, R_{k,:j} \rangle$ is the similarity of the i -th and j -th element.

At each communication round, FLESD collects the similarity matrices from a fraction C of the clients, denoted as $\mathcal{M} = \{M_k\}$, the cardinality of which is $|\mathcal{M}| = CK$. Then it ensembles the similarity matrices as follows:

$$\hat{M}_{k,ij} = \exp(M_{k,ij}/\tau_T), \forall k, i, j \quad (5)$$

$$M = \frac{1}{|\mathcal{M}|} \sum_{k=1}^m \hat{M}_k, \quad (6)$$

where τ_T is the target temperature regulating the sharpness of each local similarity matrix before averaging. The smaller τ_T is, the more spike is the similarity matrix, and the model pays more attention to the representations in a small neighborhood. In practice, τ_T needs to be smaller than 1 to achieve a good performance. Strictly speaking, the ensembled matrix M yielded by Equation 6 no longer remains a similarity matrix due to the change of the value scope, $M_{ij} \in (0, +\infty)$. However, as shown in the following section, this design is in accordance with the similarity-based knowledge distillation technique and will not be a problem.

Similarity-based distillation. Unlike traditional knowledge distillation techniques that minimize the cross-entropy between the teacher and student networks’ softened class probabilities, similarity-based distillation aims to train a student network that mimics the way the teacher network distributes a population of the representations in the feature space. Our goal is to leverage the ensemble similarity matrix as an off-line teacher network guiding the training of the student network.

Suppose a series of anchor images $\{x_{j_1}, \dots, x_{j_m}\}$ are indexed by $\{j_1, \dots, j_m\}$ where m is the size of the anchor set. For a given query image x_i and a student network f_S , the similarity between x_i and the anchor images is computed as $\{f_S(x_{j_1})^\top f_S(x_i), \dots, f_S(x_{j_m})^\top f_S(x_i)\}$. To note here that each representation $f_S(\cdot)$ is also automatically normalized

Algorithm 1: Federated self-supervised Learning via Ensemble Similarity Distillation (**FLESD**).

Procedure SERVER ()

$w^{(0)} \leftarrow$ random weight initialization

for each communication round $t = 1, \dots, T$ **do**

$S^{(t)} \leftarrow$ random subset (C fraction of the K clients)

for each client $k \in S^{(t)}$ **in parallel do**

$M_k^{(t)} \leftarrow$ CLIENTUPDATE ($k, w^{(t-1)}$)

end

$M^{(t)} \leftarrow$ ensemble from $\{M_k^{(t)}\}_{k=1}^m$

$w_0^{(t)} \leftarrow w^{(t-1)}$

for each iteration $j = 1, \dots, J$ **do**

sample a mini-batch of data from D_{pub}

update $w_j^{(t)}$ by $M^{(t)}$ through Equation 9

end

$w^{(t)} \leftarrow w_J^{(t)}$

end

return $w^{(T)}$

Procedure CLIENTUPDATE (k, w)

$w_0^{(0)} \leftarrow w^{(0)} \leftarrow w$

for each local epoch $e = 1, \dots, E$ **do**

for each training round $j = 1, \dots, J$ **do**

sample a mini-batch of data from D_k

update to $w_j^{(e)}$ through Equation 3

end

$w^{(e)} \leftarrow w_J^{(t)}$

end

$M_k \leftarrow$ similarity inference on D_{pub} with $w^{(E)}$

return M_k

to the unit-length vector as discussed before. Furthermore, we can define a probability distribution over the anchor images based on the similarity. For the student network, the probability of the i -th query on the j -th anchor is:

$$q_j^i = \frac{\exp(f_S(x_j)^\top f_S(x_i)/\tau_S)}{\sum_{u=1}^m \exp(f_S(x_{j_u})^\top f_S(x_i)/\tau_S)}, \quad (7)$$

where τ_S is the student temperature hyper parameter. We set $\tau_S = \tau_T$ following the convention of ComPress (Koohpayegani, Tejankar, and Pirsavash 2020) because this restriction assures that the probabilities of the student network and target are roughly same-scaled and have close semantic meaning. Different from ComPress and SEED (Fang et al. 2021) that have access to the teacher model, we can only perform the distillation on the similarity matrices for the sake of data privacy. The target probability p^i is retrieved from the ensembled similarity matrix M , where the i -th query’s probability over the j -th anchor is:

$$p_j^i = \frac{M_{ij}}{\sum_{k=1}^m M_{ik}}. \quad (8)$$

Finally, the global aggregation training objective L_g is the mean KL-divergence between the probabilities over the an-

| T | Linear Probing Acc. | | | | | | | | | | | | Transfer Acc. | | | |
|-----------|---------------------|-------------|---------------|--------------|-------------|---------------|---------------|-------------|---------------|--------------|-------------|---------------|-------------------------|-------------|---------------|-------------|
| | CIFAR10 | | | CIFAR100 | | | Tiny-ImageNet | | | ImageNet-100 | | | ImageNet-100 → CIFAR100 | | | |
| | $\alpha=100$ | $\alpha=1$ | $\alpha=0.01$ | $\alpha=100$ | $\alpha=1$ | $\alpha=0.01$ | $\alpha=100$ | $\alpha=1$ | $\alpha=0.01$ | $\alpha=100$ | $\alpha=1$ | $\alpha=0.01$ | $\alpha=100$ | $\alpha=1$ | $\alpha=0.01$ | |
| Non-FL | ∞ | - | 86.3 | - | - | 55.5 | - | - | 42.9 | - | - | 78.0 | - | - | 54.7 | - |
| Min-Local | 0 | 62.9 | 66.5 | 60.4 | 12.4 | 41.8 | 41.2 | 35.0 | 34.7 | 35.3 | 63.7 | 61.5 | 59.0 | 50.2 | 49.0 | 50.5 |
| FedAvg | 10 | 75.6 | 75.2 | 69.9 | 37.8 | 43.2 | 44.8 | 37.5 | 37.3 | 38.4 | 68.5 | 69.5 | 66.6 | 50.8 | 50.2 | 49.2 |
| FedProx | 10 | 71.3 | 72.3 | 67.5 | 33.9 | 39.4 | 40.6 | 25.1 | 26.0 | 26.3 | 46.1 | 44.6 | 43.2 | 33.6 | 34.0 | 34.6 |
| FLESD | 2 | 75.8 | 76.2 | 69.6 | 39.2 | 43.8 | 42.2 | 38.1 | 37.2 | 36.5 | 66.3 | 65.4 | 58.7 | 50.2 | 48.2 | 49.5 |
| FLESD-cc | 1 | 73.2 | 74.4 | 66.2 | 18.9 | 42.1 | 41.4 | 36.4 | 36.4 | 36.5 | 63.8 | 64.3 | 60.6 | 50.8 | 49.7 | 47.5 |

Table 1: Comparison with Other Federated Self-Supervised Baselines. The total epoch of local training is set as constant $E_{\text{total}}=T \times E_{\text{local}}=200$. T : communication rounds. α : value of Dirichlet distribution controlling the non-i.i.d.-ness of the clients’ data. Smaller α denotes more severe non-i.i.d.-ness. **Non-FL**: upper bound performance trained on the full dataset. **Min-Local**: lower bound performance of local training with no global aggregation. **FLESD-cc**: the degenerate form “constant communication” of FLESD. FLESD has comparable performances as the weight-averaging baseline FedAvg, but it (i) requires fewer rounds of communications; (ii) supports model-heterogeneous federated systems, and (iii) strict data privacy protection.

chor images of the target and the student network:

$$L_g(f_S) \triangleq \frac{1}{|D_{\text{pub}}|} \sum_{i=1}^{|D_{\text{pub}}|} \text{KL}(p^i \| q^i). \quad (9)$$

During the ensemble similarity distillation, the student network is constantly updated. Therefore re-computing the representations of the anchor images is required, which brings large computational overhead. To address this problem, we follow (He et al. 2020) and adopt the momentum encoder and momentum queue to maintain the recently computed representations of the anchor images. The momentum encoder is the slow version of the student network and is updated by exponential moving average (EMA). Suppose the student network f_θ is parameterized by θ and the momentum encoder f_μ is parameterized by μ . At each iteration t during ESD, we perform the following:

$$\mu^{(t+1)} = \zeta \cdot \mu^{(t)} + (1 - \zeta) \cdot \theta^{(t)}, \quad (10)$$

where ζ is the momentum encoder factor ζ controlling how slow the momentum encoder is updated towards the student network. When $\zeta = 0$, it degenerates to the case where no momentum encoder is adopted. At each step, the momentum encoder will first encode the mini-batch of the data and update the momentum queue in a first-in-first-out (FIFO) manner. This way, we spare the computational cost of forward passing the anchor images and achieve better training efficiency. We present the full algorithmic description of FLESD in Algorithm 1.

3.4 Discussion on FLESD’s Design

Why similarity matrices of the public dataset? One alternative is to send back all the representations yielded by the clients. However, since the clients have misaligned representation spaces after local training, it’s more sensible to return their geometric information. Besides, similarity matrices can be quantized for lower communication overhead. Secondly, the similarity matrix can be inferred by model of any architecture, which scales FLESD to model-heterogeneous systems. Thirdly, inferring on the

public dataset does not have privacy concerns, which strictly protects the clients’ privacy.

Why not average similarity matrices directly? One client may focus on a particular knowledge domain and has weak discriminant power on other domains due to the non-i.i.d. data distribution. Trivially averaging the similarity matrices of such clients will introduce too much noise and cause over-smoothing. Therefore we adopt exponential function with small τ_T to sharpen the similarity matrices before ensemble.

4 Empirical Experiments

4.1 Setup

Datasets and models. We benchmark our proposed framework FLESD, along with the baselines on four visual datasets, including CIFAR10/CIFAR100 (Krizhevsky, Hinton et al. 2009), Tiny-ImageNet (Le and Yang 2015), and ImageNet-100 (Tian, Krishnan, and Isola 2019a; Wang and Isola 2020). The first two datasets are composed of 32x32 RGB images; Tiny-ImageNet’s data is of size 64x64; and ImageNet-100 is 100-class subset of ImageNet and retains the original image quality. To simulate different levels of the non-i.i.d. data distribution, we set the α value of the Dirichlet distribution to $\alpha = 100, 1, 0.01$ and we benchmark all the methods on them. We use ResNet18 as the encoder network for CIFAR10/CIFAR100/Tiny-ImageNet and ResNet50 for ImageNet-100 (He et al. 2016).

Evaluation metrics. We adopt the linear probing accuracy (also known as linear evaluation) and transfer learning accuracy to evaluate the representation space quality yielded by the federated self-supervised learning frameworks (Zhang, Isola, and Efros 2016; Chen et al. 2020a; He et al. 2020). Specifically, after training, we fix the backbone network parameters and retrain a linear classifier on top of it using the entire training dataset for both metrics.

Local self-supervised training. Same local training strategy is applied to FLESD and all the baseline methods:

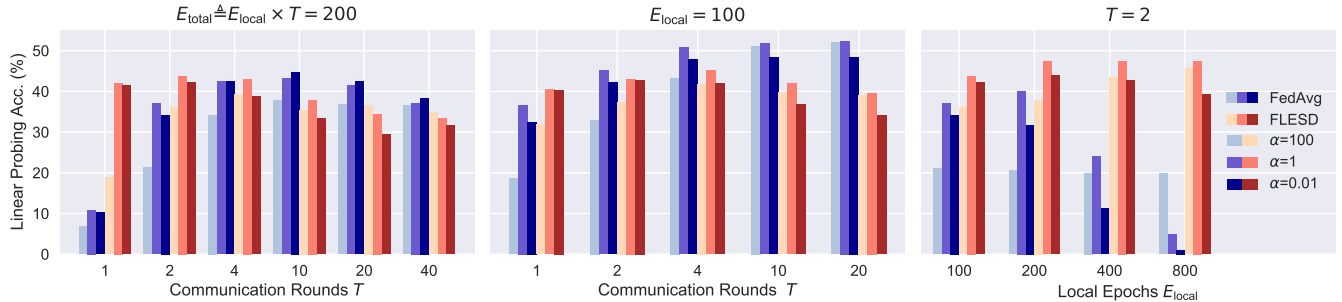


Figure 4: Influence of Different Communication Schemes, evaluated on CIFAR100. **Left:** fixed total epochs $E_{\text{total}}=200$. The performance peak of FLESD ($T=2$) appears earlier than FedAvg’s ($T=10$) in terms of communication rounds. **Middle:** fixed local epochs $E_{\text{local}}=100$. FLESD’s performance saturates as communication round increases. **Right:** fixed communication rounds $T=2$. When the communication is extremely limited, FLESD achieves better performance by increasing local training epochs. For detailed statistics, refer to Table 4 - Table 6.

trained by SimCLR framework with learning rate $\eta=1e-3$ and Adam optimizer. Batch size, temperature, and data augmentation are set differently for varying datasets for better performance. Due to the space limitation, we summarize the hyperparameters of local training in supplementary materials.

Baselines. FLESD is designed as the first federated self-supervised learning framework that scales to the model heterogeneity. We compare its performance with the classic weight-averaging-based federated methods, including FedAvg (Konecny et al. 2016) and FedProx (Li et al. 2020). We report the best performances of FedAvg in the Table 1 by fixing the total update epochs $E_{\text{total}} \triangleq T \times E_{\text{local}} = 200$ and grid-searching $T \in \{1, 2, 4, 10, 20, 40\}$. Then we train FedProx under the FedAvg’s optimal setting as described above with grid-searching $\mu \in \{0.001, 0.01, 0.1, 1\}$. Both FedAvg and FedProx’s client sampling fraction are set as $C = 1.0$.

FLESD global aggregation. In terms of global aggregation with ensemble similarity distillation, we adopt the same set of hyperparameters for all four datasets, i.e., learning rate $\eta = 1e-3$, Adam optimizer, batch size $B' = 128$, epoch $E = 200$, temperature of the target and the student network $\tau_T = \tau_S = 0.1$, factor of the momentum encoder $\zeta = 0.999$, anchor set size $m = 2048$. The augmentation scheme during the ensemble distillation phase is set the same as the corresponding augmentation used during local training. Table 1 reports the best result of FLESD by grid-searching the communication rounds $T \in \{1, 2, 4, 10, 20, 40\}$. For a fair comparison, client No.0’s data is adopted as the public dataset for the global ensemble similarity distillation, and will not be used during local training. Other federated counterparts such as FedAvg treat it as a simple client on which local training is performed. The client sampling fraction is also set to $C = 1.0$.

4.2 Comparison with Other Federated Baselines

Table 1 compares the proposed method with other federated baselines on four datasets. In general, FLESD and FedAvg both have higher linear probing accuracy than the local training lower bound on all four datasets, proving the necessity of communication and global aggregation. FLESD’s performance is comparable to the federated baseline FedAvg on

multiple datasets, on some of which is even better. It showcases the effectiveness of our method. What’s more, FLESD achieves this with significantly fewer communication round ($T=2$ vs $T=10$), demonstrating its communication-efficient property. However, the gap between the federated learning methods and the upper bound performance which is quite large: on CIFAR10/CIFAR100/ImageNet-100, the gaps are over 10 points, which needs to be addressed in the future.

4.3 Case Studies

Communication rounds. For completeness, we study three different types of the communication schemes as in Figure 4. Firstly, when the total epochs is set as constant $E_{\text{total}} = 200$ (left subfigure of Figure 4), we iterate through the set of communication rounds and compare the difference between FLESD and the FedAvg baseline. Both methods’ performance curve is of a reversed U-shape. The performance peak of FLESD appears earlier than FedAvg, which showcases the communication-efficiency of our proposed framework. Secondly, we fix the local training epochs as $E_{\text{local}} = 100$ and allow the model to conduct more communication rounds up to 20 (middle subfigure of Figure 4). There are two takeaways: (i) though the local training epochs in federated supervised learning are normally set to 5-10, FedAvg performs surprisingly well when trained longer on the local clients. This phenomenon can be partially explained by the observed robustness in Section 2; (ii) FLESD’s performance quickly saturates as the communication rounds increases, which implies possible future improvements. Thirdly, we consider the case where the learning system’s communication is strictly limited ($T=2$), FLESD’s performance is improved as the local training epochs increase. However, except the case when the local data is i.i.d. ($\alpha = 100$), FedAvg gradually fails as the local training epochs increases. This phenomenon shows that our method is improved by better-quality of local training, and disputes potential opposition that FLESD simply trains self-supervised model on the public dataset.

Temperatures (τ_T, τ_S). Though engineeringly speaking, it’s feasible to set the temperatures τ_T and τ_S differently (Fang et al. 2021), we set them the same so that the similarity distribution of the ensembled targets are of the

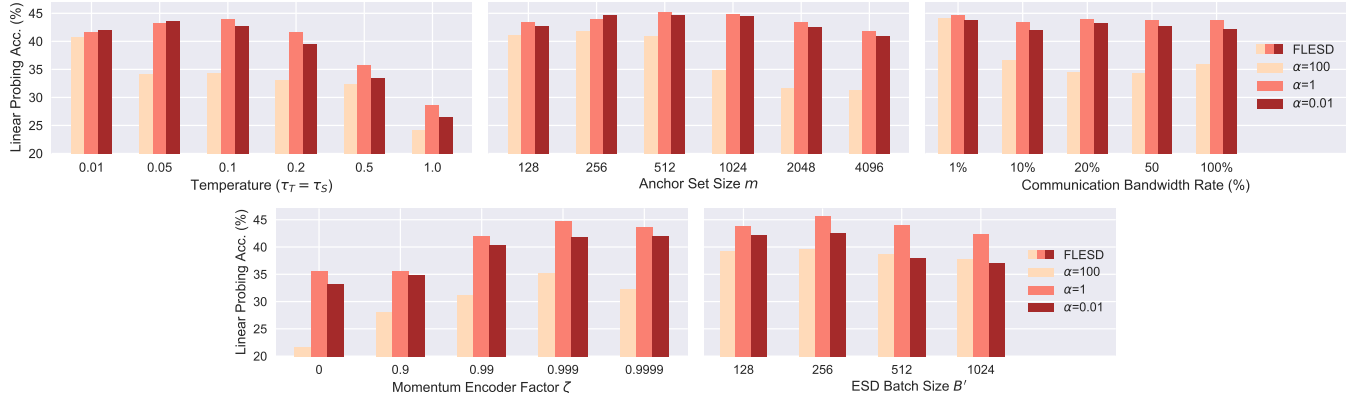


Figure 5: Case Studies on FLESD, evaluated on CIFAR100. **Upper-Left:** influence of the ESD temperatures, where τ_S is set equal to τ_T . High temperature causes severe performance drop. **Upper-Middle:** influence of the anchor set size m . FLESD is not monotonically improved with the increasing anchor set size. **Upper-Right:** influence of similarity matrix quantization. FLESD’s final performance remains stable in terms of quantization rate change. It achieves better performance with lower communication cost. **Lower-Left:** influence of momentum encoder factor ζ . When the momentum encoder is removed ($\zeta = 0$), the performance of FLESD is greatly undermined. **Lower-Right:** influence of the ESD batch size. Larger batch size leads to more global and complete focus on the geometry of the ensemble representation space. However, it does not necessarily cause performance boost. Refer to Table 7 - Table 11 for the statistics.

same scale as that of the student network (Koohpayegani, Tejankar, and Pirsavash 2020). We iterate through the temperature setting in $\{0.01, 0.05, 0.1, 0.2, 0.5, 1.0\}$. In general, the temperature τ_T controls the range of the neighborhood the ensembled similarity matrix pays attention to. The lower the τ_T , the tighter the clusters of the representation distribution are. As shown in the upper-left subfigure of Figure 5, the impact of the temperature is also U-shaped: increasing the temperature would cause the distribution over-smoothed. Finally, $\tau_T = \tau_S = 0.1$ is adopted as default.

Anchor set size m . In the work that adopts similarity-based distillation (Koohpayegani, Tejankar, and Pirsavash 2020; Fang et al. 2021), normally larger anchor image set (momentum queue) brings better performance of the distilled model. However, in the case of FLESD, there exists a trade-off (upper-middle subfigure of Figure 5). Increasing the anchor set size from 128 to 512 improves the linear evaluation accuracy, while further enlarging it causes severe performance drop. We conjecture the cause might be the slow update of the early representations in the momentum queue, therefore enlarging the queue size brings more noises.

Similarity matrix quantization. Further optimization on the communication bandwidth can be made for FLESD. In distillation-based federated supervised learning methods, quantization of the predicted logits is applied for faster communication with subtle performance drops (Sattler et al. 2020). Similarly, to achieve lower-cost communication, we can quantize the similarity matrices by preserving $n\%$ of the most similar samples’ values for each entry, and substitute the discarded values with 0. Surely it will damage the symmetry of the original similarity matrix, while it doesn’t affect the following ensemble and similarity distillation process. We report the result in the upper-right subfigure of Figure 5.

Different from supervised learning, quantization even has positive influence on FLESD’s performance as only 1% of the similarity values are preserved. Compared to the exponential function, which is a soft way to sharpen the distribution, quantization is a hard sharpening method and thus can affect the model’s performance in a different way from the supervised learning framework.

Momentum Encoder Factor ζ . In this subsection, we want to validate the necessity of the momentum encoder. We study how the factor ζ affects FLESD’s performance by iterating through $\zeta \in \{0, 0.9, 0.99, 0.999, 0.9999\}$. We show the results in the lower right subfigure of Figure 5. The influence of ζ is also reversely U-shaped. Especially when $\zeta = 0$, FLESD’s performance drops by a large margin. The sweet spot is achieved at $\zeta = 0.999$. Therefore we adopt this setting as default.

EDS Batch Size B' . During the ensemble similarity distillation, large batch size decreases the randomness of the optimization. Therefore it focuses more on the global geometry of the representation space during optimization. For the sake of fair comparison, we set the iteration numbers of training as constant. In the main experiments, we adopt $B' = 128$ as the default setting. However, the lower-right subfigure of Figure 5 shows that slightly increasing the batch size to $B' = 256$ is conducive to improving the FLESD’s performance, but further increasing B' will do the opposite.

Public dataset. We study three different degrees of the public data heterogeneity. The federated self-supervised training FLESD is conducted with the public dataset consisting of CIFAR100 (in-domain), CIFAR10 (similar-domain), and Tiny-ImageNet (out-of-domain), respectively. To note here, we sample the public data uniformly on all the semantic classes to compose the public dataset, and all the other

| α | CIFAR100 | | | CIFAR10 | | | Tiny-ImageNet | | |
|----------|-------------|-------------|-------------|-------------|-------------|-------------|---------------|-------------|-------------|
| | 100 | 1 | 0.01 | 100 | 1 | 0.01 | 100 | 1 | 0.01 |
| 1% | 16.3 | 18.3 | 18.8 | 13.5 | 16.7 | 15.9 | 17.5 | 20.6 | 21.0 |
| 5% | 31.7 | 36.2 | 37.2 | 25.9 | 35.0 | 34.9 | 24.8 | 29.8 | 30.1 |
| 10% | 38.7 | 41.8 | 43.2 | 34.3 | 38.2 | 39.2 | 28.7 | 29.3 | 31.5 |
| 20% | 41.3 | 46.1 | 46.6 | 38.8 | 41.3 | 41.9 | 27.8 | 30.3 | 30.4 |

Table 2: Study on the Public Dataset, where local training and evaluation are performed on CIFAR100.

hyperparamters are set the same as the main experiment. As shown in Table 2, the performance of the final aggregated model increases as the public dataset includes more samples, while the FLESD model that adopts the out-of-domain public dataset approaches to saturation more quickly then the in-domain and similar-domain dataset.

Convergence of FLESD. We train FLESD and the baseline method FedAvg for longer total epochs $E_{\text{total}}=2000$ to understand its convergence. Due to the fact that FLESD favors fewer communication rounds while FedAvg favors more, here we set $T=5$ and $T=20$ respectively. The self-supervised training loss is reported in Figure 6. As shown in the figure, the overall tendency of FLESD’s training loss is similar to FedAvg. However, after each round of global aggregation, the model is a bit diverged from the optimal point of the self-supervised contrastive loss on the clients. This phenomenon indicates that the model of FLESD might have a looser bound on the self-supervised training object, which needs to be further studied and improved.

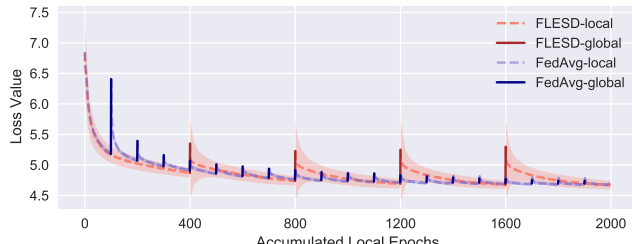


Figure 6: Training Loss Trajectories, evaluated on CIFAR100, $\alpha=1$. Dashed lines denote the clients’ averaged local training losses. Solid lines denote global aggregation.

5 Related Work

Federated Learning. Firstly proposed by (Konecny et al. 2016) for jointly training machine learning models across clients while preserving their data privacy, federated learning has become a key research area in distributed machine learning. One important challenge of federated learning is the non-i.i.d. data distribution and many works have been proposed to particularly address this problem (Zhao et al. 2018; Li et al. 2020, 2021; Wang et al. 2020). Another focus is to solve model heterogeneity. Smith et al. (2018) is the first attempt trying to apply multi-task learning framework to aggregate separated but related models; FedMD (Li and Wang 2019) introduces the technique of knowledge distillation (Hinton, Vinyals, and Dean 2015) to federated

learning for client personalization; FedDF proposes to use ensemble distillation to effectively aggregate the clients’ knowledge regardless of the model architectures. Different from the methods above that address federated supervised learning, FLESD aims at solving the model-agnostic federated learning without labels using ensemble similarity distillation.

Self-Supervised Contrastive Learning. As discussed in Section 3, contrastive learning follows the multi-view hypothesis and performs instance discrimination pretext task to train the encoder network (Wu et al. 2018; Oord, Li, and Vinyals 2018; Tian, Krishnan, and Isola 2019a; Chen et al. 2020a; He et al. 2020). There are some works that explore self-supervised learning in federated scenario (Jin et al. 2020; van Berlo, Saeed, and Ozcelebi 2020; Zhang et al. 2020). FedCA proposes to use a public dataset and an alignment module to address the problem of representation misalignment of FedAvg applied to SimCLR (Zhang et al. 2020). However, it fails to notice the non-i.i.d. robustness of the self-supervised model and does not solve the problem of model heterogeneity. To the best of our knowledge, we are the first to handle the challenge of model heterogeneity in federated self-supervised learning.

Knowledge Distillation. The technique of Knowledge Distillation (KD) was firstly proposed to train a lightweight model under the guidance of a pre-trained high-capacity model (Hinton, Vinyals, and Dean 2015). Up to today, there are generally three categories of distillation methods: response-based distillation (Hinton, Vinyals, and Dean 2015), feature-based distillation (Romero et al. 2014; Zagoruyko and Komodakis 2016; Kim, Park, and Kwak 2018; Heo et al. 2019; Tian, Krishnan, and Isola 2019b), and relation-based distillation (Park et al. 2019; Lassance et al. 2020; Koohpayegani, Tejankar, and Pirsavash 2020; Fang et al. 2021). Our designed global aggregation is directly inspired by CompRes (Koohpayegani, Tejankar, and Pirsavash 2020) and SEED (Fang et al. 2021), which distill the knowledge from a pre-trained model by matching the similarity distribution. However, there are two significant differences between the previous work and our method FLESD. Firstly, due to the data privacy concerns, we do not have direct access to the teacher model, and thus we have to perform the distillation on a “off-line” manner. Secondly, we have multiple teacher models that are trained under different local data distributions, and we ensemble their similarity matrices to form a global distillation target.

6 Conclusion

This paper proposes a federated self-supervised learning framework that applies to model-heterogeneous systems and strict privacy protection protocol that doesn’t allow global aggregation with model weights. The proposed method FLESD adopts the technique of ensemble similarity distillation to aggregate the clients’ learned knowledge at each communication round. The similarity distillation is conducted on a public dataset that is free of privacy concerns. Besides its wider range of application, FLESD is more communication-efficient than the existing frameworks.

References

Chen, T.; Kornblith, S.; Norouzi, M.; and Hinton, G. 2020a. A simple framework for contrastive learning of visual representations. In *International conference on machine learning*, 1597–1607. PMLR.

Chen, T.; Kornblith, S.; Swersky, K.; Norouzi, M.; and Hinton, G. 2020b. Big self-supervised models are strong semi-supervised learners. *arXiv preprint arXiv:2006.10029*.

Chen, X.; Fan, H.; Girshick, R.; and He, K. 2020c. Improved baselines with momentum contrastive learning. *arXiv preprint arXiv:2003.04297*.

Chen, X.; and He, K. 2020. Exploring Simple Siamese Representation Learning. *arXiv preprint arXiv:2011.10566*.

Chen, X.; Xie, S.; and He, K. 2021. An empirical study of training self-supervised vision transformers. *arXiv preprint arXiv:2104.02057*.

Fang, Z.; Wang, J.; Wang, L.; Zhang, L.; Yang, Y.; and Liu, Z. 2021. Seed: Self-supervised distillation for visual representation. *arXiv preprint arXiv:2101.04731*.

Grill, J.-B.; Strub, F.; Altché, F.; Tallec, C.; Richemond, P. H.; Buchatskaya, E.; Doersch, C.; Pires, B. A.; Guo, Z. D.; Azar, M. G.; et al. 2020. Bootstrap your own latent: A new approach to self-supervised learning. *arXiv preprint arXiv:2006.07733*.

He, K.; Fan, H.; Wu, Y.; Xie, S.; and Girshick, R. 2020. Momentum contrast for unsupervised visual representation learning. In *Proceedings of the IEEE/CVF Conference on Computer Vision and Pattern Recognition*, 9729–9738.

He, K.; Zhang, X.; Ren, S.; and Sun, J. 2016. Deep residual learning for image recognition. In *Proceedings of the IEEE conference on computer vision and pattern recognition*, 770–778.

Heo, B.; Lee, M.; Yun, S.; and Choi, J. Y. 2019. Knowledge transfer via distillation of activation boundaries formed by hidden neurons. In *Proceedings of the AAAI Conference on Artificial Intelligence*, volume 33, 3779–3787.

Hinton, G.; Vinyals, O.; and Dean, J. 2015. Distilling the knowledge in a neural network. *arXiv preprint arXiv:1503.02531*.

Jin, Y.; Wei, X.; Liu, Y.; and Yang, Q. 2020. Towards utilizing unlabeled data in federated learning: A survey and prospective. *arXiv preprint arXiv:2002.11545*.

Kim, J.; Park, S.; and Kwak, N. 2018. Paraphrasing complex network: Network compression via factor transfer. *arXiv preprint arXiv:1802.04977*.

Kingma, D. P.; and Ba, J. 2014. Adam: A method for stochastic optimization. *arXiv preprint arXiv:1412.6980*.

Konecny, J.; McMahan, H. B.; Yu, F. X.; Richtárik, P.; Suresh, A. T.; and Bacon, D. 2016. Federated learning: Strategies for improving communication efficiency. *arXiv preprint arXiv:1610.05492*.

Koohpayegani, S. A.; Tejankar, A.; and Pirsavash, H. 2020. Compress: Self-supervised learning by compressing representations. *arXiv preprint arXiv:2010.14713*.

Krizhevsky, A.; Hinton, G.; et al. 2009. Learning multiple layers of features from tiny images.

Lassance, C.; Bontonou, M.; Hacene, G. B.; Gripon, V.; Tang, J.; and Ortega, A. 2020. Deep geometric knowledge distillation with graphs. In *ICASSP 2020-2020 IEEE International Conference on Acoustics, Speech and Signal Processing (ICASSP)*, 8484–8488. IEEE.

Le, Y.; and Yang, X. 2015. Tiny imagenet visual recognition challenge. *CS 231N*, 7(7): 3.

Li, D.; and Wang, J. 2019. FedMD: Heterogenous Federated Learning via Model Distillation. *arXiv:1910.03581*.

Li, T.; Sahu, A. K.; Zaheer, M.; Sanjabi, M.; Talwalkar, A.; and Smith, V. 2020. Federated Optimization in Heterogeneous Networks. *arXiv:1812.06127*.

Li, X.; Jiang, M.; Zhang, X.; Kamp, M.; and Dou, Q. 2021. FedBN: Federated Learning on Non-IID Features via Local Batch Normalization. *arXiv:2102.07623*.

Lin, T.; Kong, L.; Stich, S. U.; and Jaggi, M. 2020. Ensemble distillation for robust model fusion in federated learning. *arXiv preprint arXiv:2006.07242*.

McMahan, B.; Moore, E.; Ramage, D.; Hampson, S.; and y Arcas, B. A. 2017. Communication-efficient learning of deep networks from decentralized data. In *Artificial Intelligence and Statistics*, 1273–1282. PMLR.

Oord, A. v. d.; Li, Y.; and Vinyals, O. 2018. Representation learning with contrastive predictive coding. *arXiv preprint arXiv:1807.03748*.

Park, W.; Kim, D.; Lu, Y.; and Cho, M. 2019. Relational knowledge distillation. In *Proceedings of the IEEE/CVF Conference on Computer Vision and Pattern Recognition*, 3967–3976.

Romero, A.; Ballas, N.; Kahou, S. E.; Chassang, A.; Gatta, C.; and Bengio, Y. 2014. Fitnets: Hints for thin deep nets. *arXiv preprint arXiv:1412.6550*.

Sattler, F.; Marban, A.; Rischke, R.; and Samek, W. 2020. Communication-efficient federated distillation. *arXiv preprint arXiv:2012.00632*.

Smith, V.; Chiang, C.-K.; Sanjabi, M.; and Talwalkar, A. 2018. Federated Multi-Task Learning. *arXiv:1705.10467*.

Tian, Y.; Krishnan, D.; and Isola, P. 2019a. Contrastive multiview coding. *arXiv preprint arXiv:1906.05849*.

Tian, Y.; Krishnan, D.; and Isola, P. 2019b. Contrastive representation distillation. *arXiv preprint arXiv:1910.10699*.

van Berlo, B.; Saeed, A.; and Ozcelebi, T. 2020. Towards federated unsupervised representation learning. In *Proceedings of the Third ACM International Workshop on Edge Systems, Analytics and Networking*, 31–36.

Wang, H.; Yurochkin, M.; Sun, Y.; Papailiopoulos, D.; and Khazaeni, Y. 2020. Federated Learning with Matched Averaging. *arXiv:2002.06440*.

Wang, T.; and Isola, P. 2020. Understanding contrastive representation learning through alignment and uniformity on the hypersphere. In *International Conference on Machine Learning*, 9929–9939. PMLR.

Wu, Z.; Xiong, Y.; Yu, S.; and Lin, D. 2018. Unsupervised feature learning via non-parametric instance-level discrimination. *arXiv preprint arXiv:1805.01978*.

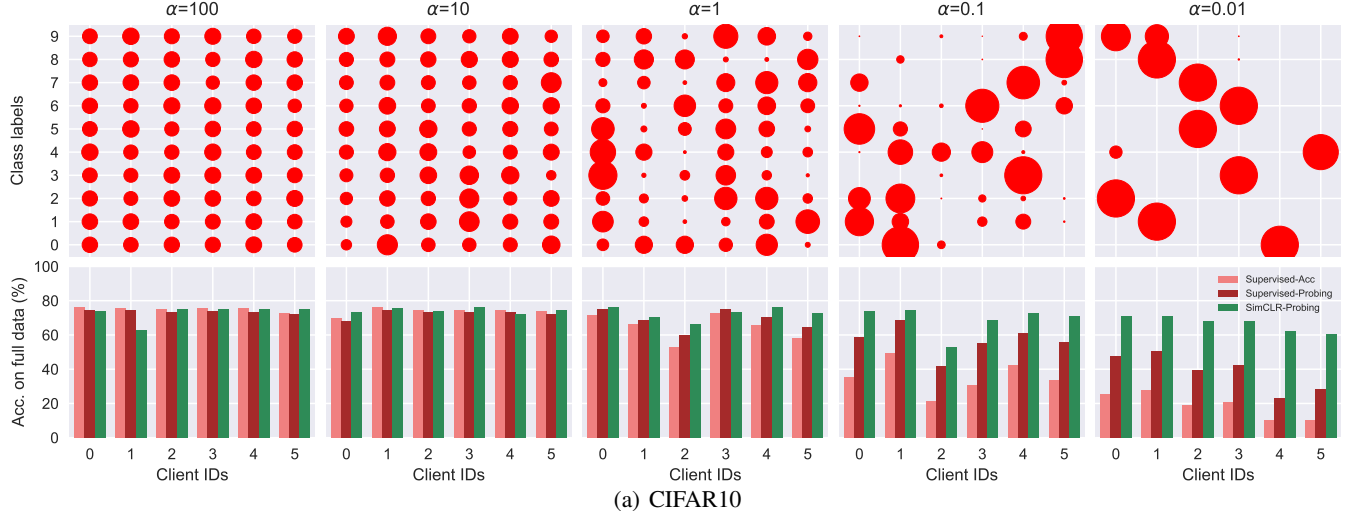
Zagoruyko, S.; and Komodakis, N. 2016. Paying more attention to attention: Improving the performance of convolutional neural networks via attention transfer. *arXiv preprint arXiv:1612.03928*.

Zbontar, J.; Jing, L.; Misra, I.; LeCun, Y.; and Deny, S. 2021. Barlow twins: Self-supervised learning via redundancy reduction. *arXiv preprint arXiv:2103.03230*.

Zhang, F.; Kuang, K.; You, Z.; Shen, T.; Xiao, J.; Zhang, Y.; Wu, C.; Zhuang, Y.; and Li, X. 2020. Federated Unsupervised Representation Learning. *arXiv:2010.08982*.

Zhang, R.; Isola, P.; and Efros, A. A. 2016. Colorful image colorization. In *European conference on computer vision*, 649–666. Springer.

Zhao, Y.; Li, M.; Lai, L.; Suda, N.; Civin, D.; and Chandra, V. 2018. Federated learning with non-iid data. *arXiv preprint arXiv:1806.00582*.



(a) CIFAR10

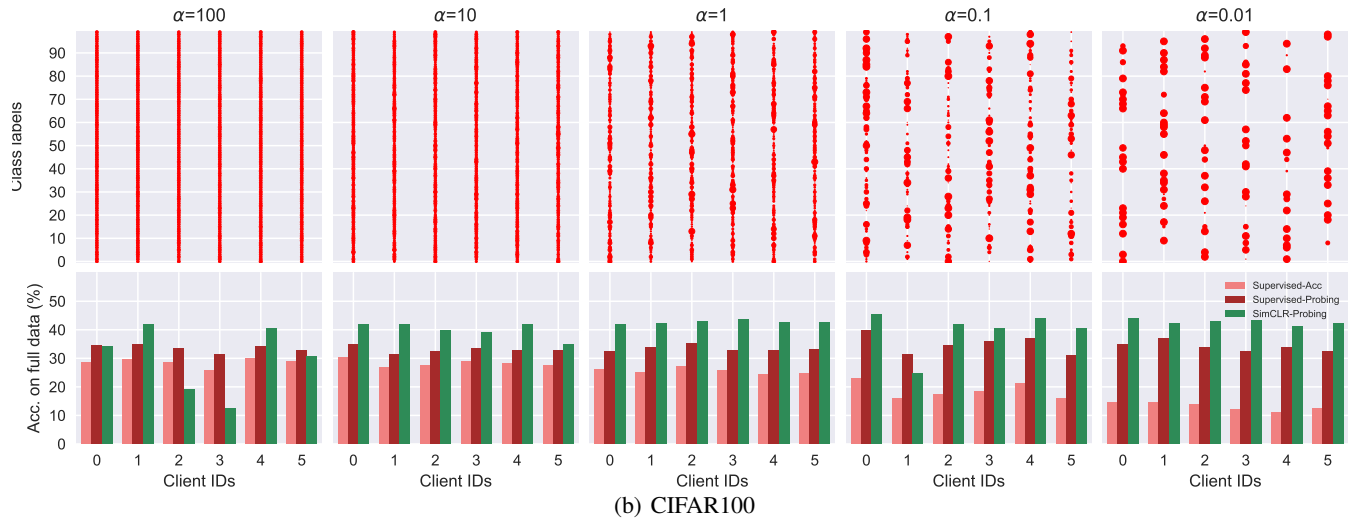


Figure 7: Local training of supervised and self-supervised learning on CIFAR10/100. The top row of both subfigures visualizes the non-i.i.d.-ness of the data distribution; the radius of each circle represents the size of the local dataset. The bottom row compares the behavior of supervised and self-supervised local training. The self-supervised framework SimCLR is more robust than the supervised method. For CIFAR10, the performance deterioration happens especially at $\alpha=0.01$ for supervised learning paradigm, where client No.4 and No.5 hold only single category of the data. This phenomenon, however, is not apparent in CIFAR100 since the number of semantic classes significantly surpasses the number of the clients and the situation of one client holding single dangling class doesn't occur.

| Dataset | Method | Evaluation | Non-i.i.d-ness α | Client ID | | | | | | Mean | Min |
|---------------|------------|--------------|-------------------------|-----------|------|------|------|------|------|------|------|
| | | | | C0 | C1 | C2 | C3 | C4 | C5 | | |
| CIFAR10 | Supervised | Acc. | 100 | 76.1 | 75.7 | 75.2 | 75.5 | 75.4 | 72.5 | 75.1 | 72.5 |
| | | | 10 | 69.5 | 76.2 | 74.7 | 74.5 | 74.3 | 73.8 | 73.8 | 69.5 |
| | | | 1 | 71.8 | 66.2 | 52.9 | 72.5 | 65.7 | 57.9 | 64.5 | 52.9 |
| | | | 0.1 | 35.6 | 49.5 | 21.4 | 30.8 | 42.4 | 33.5 | 35.5 | 21.4 |
| | | | 0.01 | 25.6 | 27.8 | 18.9 | 20.6 | 10.0 | 10.0 | 18.8 | 10.0 |
| | SimCLR | Linear Probe | 100 | 74.7 | 74.3 | 73.0 | 73.6 | 73.3 | 72.1 | 73.5 | 72.1 |
| | | | 10 | 67.9 | 74.7 | 73.0 | 73.5 | 73.3 | 72.3 | 72.5 | 67.9 |
| | | | 1 | 75.1 | 68.5 | 60.1 | 74.8 | 70.1 | 64.4 | 68.8 | 60.1 |
| | | | 0.1 | 58.9 | 68.6 | 41.8 | 54.9 | 60.9 | 56.0 | 56.9 | 41.8 |
| | | | 0.01 | 47.8 | 50.8 | 39.3 | 42.5 | 23.0 | 28.4 | 38.6 | 23.0 |
| CIFAR100 | Supervised | Acc. | 100 | 74.0 | 62.9 | 74.8 | 75.0 | 75.1 | 75.0 | 72.8 | 62.9 |
| | | | 10 | 73.1 | 75.4 | 73.6 | 76.1 | 72.0 | 74.3 | 74.1 | 72.0 |
| | | | 1 | 76.3 | 70.3 | 66.5 | 73.5 | 76.0 | 72.9 | 72.6 | 66.5 |
| | | | 0.1 | 73.8 | 74.5 | 52.6 | 68.5 | 72.8 | 71.0 | 68.9 | 52.6 |
| | | | 0.01 | 70.7 | 70.8 | 68.1 | 67.8 | 62.4 | 60.4 | 66.7 | 60.4 |
| | SimCLR | Linear Probe | 100 | 28.5 | 29.6 | 28.5 | 25.9 | 29.8 | 28.8 | 28.5 | 25.9 |
| | | | 10 | 30.3 | 26.7 | 27.5 | 28.9 | 28.3 | 27.5 | 28.2 | 26.7 |
| | | | 1 | 26.2 | 24.9 | 27.1 | 25.6 | 24.4 | 24.7 | 25.5 | 24.4 |
| | | | 0.1 | 23.0 | 16.0 | 17.4 | 18.3 | 21.1 | 16.1 | 18.7 | 16.0 |
| | | | 0.01 | 14.4 | 14.5 | 13.9 | 12.1 | 11.2 | 12.4 | 13.1 | 11.2 |
| Tiny-ImageNet | SimCLR | Linear Probe | 100 | 34.4 | 34.7 | 33.4 | 31.2 | 34.0 | 32.7 | 33.4 | 31.2 |
| | | | 10 | 35.0 | 31.5 | 32.5 | 33.3 | 32.7 | 32.6 | 32.9 | 31.5 |
| | | | 1 | 32.5 | 33.7 | 35.3 | 32.8 | 32.9 | 33.0 | 33.4 | 32.5 |
| | | | 0.1 | 39.7 | 31.3 | 34.6 | 35.8 | 37.0 | 30.9 | 34.9 | 31.3 |
| | | | 0.01 | 35.0 | 36.8 | 33.7 | 32.5 | 33.7 | 32.4 | 34.0 | 32.4 |
| | SimCLR | Linear Probe | 100 | 34.0 | 41.7 | 19.2 | 12.4 | 40.6 | 30.6 | 29.8 | 12.4 |
| | | | 10 | 41.8 | 41.9 | 39.6 | 38.9 | 41.9 | 34.9 | 39.8 | 34.9 |
| | | | 1 | 41.8 | 42.3 | 43.0 | 43.5 | 42.6 | 42.7 | 42.7 | 41.8 |
| | | | 0.1 | 45.5 | 24.8 | 41.7 | 40.6 | 43.8 | 40.4 | 39.5 | 24.8 |
| | | | 0.01 | 44.0 | 42.3 | 42.8 | 43.2 | 41.2 | 42.3 | 42.6 | 41.2 |
| ImageNet-100 | SimCLR | Linear Probe | 100 | 35.5 | 35.0 | 35.4 | 35.5 | 35.6 | 35.0 | 35.3 | 35.0 |
| | | | 1 | 36.3 | 34.7 | 35.4 | 35.4 | 35.6 | 35.9 | 35.6 | 34.7 |
| | | | 0.01 | 36.2 | 35.6 | 34.6 | 36.1 | 35.3 | 35.8 | 35.6 | 35.3 |

Table 3: Local training of supervised/self-supervised learning on 4 different datasets with different degrees of non-i.i.d.-ness. Both methods are fully evaluated on CIFAR10/CIFAr100. For Tiny-ImageNet and ImageNet, we provide self-supervised method SimCLR’s performances that is used in the main body of our paper.

| | Non-i.i.d.-ness α | Communication Rounds T | | | | | |
|--------|--------------------------|--------------------------|------|------|------|------|------|
| | | 1 | 2 | 4 | 10 | 20 | 40 |
| FedAvg | 100 | 6.8 | 21.3 | 34.2 | 37.8 | 36.8 | 36.6 |
| | 1 | 10.9 | 37.0 | 42.5 | 43.2 | 41.5 | 37.2 |
| | 0.01 | 10.3 | 34.2 | 42.5 | 44.8 | 42.4 | 38.4 |
| FLESD | 100 | 18.9 | 36.0 | 39.2 | 35.4 | 36.7 | 34.8 |
| | 1 | 42.1 | 43.8 | 43.0 | 37.9 | 34.4 | 33.4 |
| | 0.01 | 41.4 | 42.2 | 38.8 | 33.3 | 29.4 | 31.6 |

Table 4: Influence of the communication rounds with total epochs set constant $E_{\text{total}}=200$, evaluated on CIFAR100.

| | Non-i.i.d.-ness α | Communication Rounds T | | | | | | | | | | | |
|--------|--------------------------|--------------------------|------|------|------|------|------|------|------|------|------|------|------|
| | | 1 | 2 | 3 | 4 | 5 | 6 | 7 | 8 | 9 | 10 | 15 | 20 |
| FedAvg | 100 | 18.6 | 33.0 | 39.2 | 43.3 | 46.2 | 47.9 | 49.2 | 50 | 50.7 | 51.2 | 51.4 | 52.0 |
| | 1.0 | 36.7 | 45.2 | 48.6 | 50.8 | 51.2 | 51.4 | 51.6 | 51.7 | 51.8 | 52.1 | 52.6 | 52.4 |
| | 0.01 | 32.5 | 42.2 | 46.8 | 47.9 | 48.6 | 48.3 | 48.4 | 48.3 | 48.4 | 48.3 | 48.4 | 48.4 |
| FLESD | 100 | 31.9 | 37.4 | 40.0 | 41.8 | 41.6 | 41.6 | 41.3 | 40.9 | 40.5 | 39.8 | 39.0 | 39.1 |
| | 1 | 40.5 | 43.0 | 44.4 | 45.1 | 44.5 | 44.0 | 43.1 | 42.7 | 42.4 | 41.9 | 40.5 | 39.6 |
| | 0.01 | 40.3 | 42.8 | 43.0 | 42.0 | 41.1 | 40.0 | 38.6 | 38.3 | 37.5 | 36.8 | 35.1 | 34.1 |

Table 5: Influence of the communication rounds with local epochs set constant $E_{\text{local}}=100$, evaluated on CIFAR100.

| | Non-i.i.d.-ness α | Local Epochs E_{local} | | | |
|--------|--------------------------|---------------------------------|------|------|------|
| | | 100 | 200 | 400 | 800 |
| FedAvg | 100 | 21.0 | 20.6 | 20.0 | 19.9 |
| | 1 | 37.0 | 40.1 | 24.0 | 4.8 |
| | 0.01 | 34.2 | 31.8 | 11.3 | 1.0 |
| FLESD | 100 | 36.0 | 37.9 | 43.4 | 45.6 |
| | 1 | 43.8 | 47.3 | 47.5 | 47.5 |
| | 0.01 | 42.2 | 43.9 | 42.7 | 39.3 |

Table 6: Influence of the local training epochs with communication rounds restricted to $T=2$, evaluated on CIFAR100.

| Non-i.i.d.-ness α | Percentage of Similarity Matrix Preserved (%). | | | | |
|--------------------------|--|------|------|------|------|
| | 1% | 10% | 20% | 50% | 100% |
| 100 | 44.2 | 36.7 | 34.6 | 34.4 | 36.0 |
| 1 | 44.6 | 43.5 | 44.0 | 43.7 | 43.8 |
| 0.01 | 43.7 | 42.0 | 43.3 | 42.8 | 42.2 |

Table 7: FLESD case study on **Similarity Matrix Quantization**, evaluated on CIFAR100.

| Non-i.i.d.-ness α | Ensemble Similarity Distillation Temperatures $\tau_T = \tau_S$ | | | | | |
|--------------------------|---|------|------|------|------|------|
| | 0.01 | 0.05 | 0.1 | 0.2 | 0.5 | 1.0 |
| 100 | 40.7 | 34.2 | 34.4 | 33.1 | 32.4 | 24.2 |
| 1 | 41.6 | 43.3 | 44.0 | 41.7 | 35.8 | 28.7 |
| 0.01 | 42.0 | 43.6 | 42.8 | 39.5 | 33.4 | 26.5 |

Table 8: FLESD case study on **Ensemble Similarity Distillation Temperatures**, evaluated on CIFAR100.

| Non-i.i.d.-ness α | Anchor Set Size m | | | | | |
|--------------------------|---------------------|------|------|------|------|------|
| | 128 | 256 | 512 | 1024 | 2048 | 4096 |
| 100 | 41.2 | 41.9 | 41.0 | 34.9 | 31.7 | 31.3 |
| 1 | 43.5 | 44.0 | 45.2 | 44.8 | 43.4 | 41.8 |
| 0.01 | 42.7 | 44.7 | 44.6 | 44.5 | 42.6 | 41.0 |

Table 9: FLESD case study on **Anchor Set Size m** , evaluated on CIFAR100.

| Non-i.i.d.-ness α | Momentum Encoder Factor ζ | | | | |
|--------------------------|---------------------------------|------|------|-------|--------|
| | 0 | 0.9 | 0.99 | 0.999 | 0.9999 |
| 100 | 21.7 | 28.0 | 31.2 | 35.1 | 32.2 |
| 1 | 35.5 | 35.5 | 42.0 | 44.8 | 43.6 |
| 0.01 | 33.1 | 34.9 | 40.4 | 41.7 | 41.9 |

Table 10: FLESD case study on **Momentum Encoder Factor ζ** , evaluated on CIFAR100.

| Non-i.i.d.-ness α | Batch Size of FLESD | | | |
|--------------------------|---------------------|------|------|------|
| | 128 | 256 | 512 | 1024 |
| 100 | 39.2 | 39.5 | 38.7 | 37.8 |
| 1 | 43.8 | 45.7 | 44.0 | 42.3 |
| 0.01 | 42.2 | 42.5 | 38.0 | 37.1 |

Table 11: FLESD case study on **Batch Size of FLESD**, evaluated on CIFAR100.